Structural Relaxations of Thin Polymer Films

Bradley Frieberg, Emmanouil Glynos, and Peter F. Green

Phys. Rev. Lett. **108**, 268304 — Published 26 June 2012

DOI: 10.1103/PhysRevLett.108.268304

Structural relaxations of thin polymer films

Bradley Frieberg[1], Emmanouil Glynos[2], Peter F. Green[1,2,3]

[1]Macromolecular Science and Engineering Program, [2]Departments of Material Science and Engineering, [3]Chemical Engineering, University of Michigan, Ann Arbor, Michigan 48109, USA

ABSTRACT

Time-dependent changes of thermodynamic properties due to structural relaxations, physical aging, occur in all glasses. We show that the physical aging of thin supported films of star-shaped macromolecules, with f arms of length N_{arm}, exhibit average aging dynamics that are sensitive to f and N_{arm}. Regions of the films in proximity to interfaces age at substantially different rates than the interior of the film; this is also true of linear chain systems. This behavior may be reconciled in terms of a universal "picture" that accounts only for changes in the local T_g of the films.

When a liquid is quenched at a sufficiently rapid rate to a temperature T below its glass transition temperature, T_g, it forms a glass. Some systems, such as atactic polymers, by virtue of their molecular structure, form glasses upon solidification, regardless of quenching rates. In this non-ergodic state, at $T<T_g$, the material possesses excess thermodynamic properties. At such a temperature, the glass structurally relaxes toward equilibrium, accompanied by time dependent changes in physical properties.[1-4] This phenomenon, known as physical aging. The long-term structural stability of glasses, regardless of chemical structure, is important for their functionality and reliability in different technologies.

The driving force for physical aging depends on the difference between T_g and the temperature T_{age}, $\Delta T_A=T_{age}-T_g$, at which the sample is held during aging. The aging rate, β, is zero when $\Delta T_A\approx 0$ and increases with increasing magnitude of ΔT_A; it exhibits a maximum before approaching zero again as ΔT_A is increased further.[5-7] The maximum is believed to be due to a competition between the increasing driving force for aging, ΔT_A, with decreasing temperature and the thermally activated molecular relaxations that accommodate the recovery of the system, which decrease with decreasing aging temperature, T_{age}.[8]

While the phenomenon of aging has been studied in the bulk for decades,[1, 4, 7, 9] there has recently been a keen interest in thin polymer films, for both scientific and technological reasons.[2, 6, 10] The challenge associated with thin films is that the interfaces (substrates or free surface) influence the local monomer segmental packing

density, and configurational entropies.[11-15] A natural consequence of such effects associated with monomer-interface interactions is that the average T_g of polymer thin films is a function of its thickness H; this thickness dependence is well documented by experiment,[16-18] theory and simulations.[11-15, 19] For thin supported films of linear chains on a non-wetting substrate, e.g. polystyrene (PS) on silicon oxide (PS/SiO_x), [18-21] the average glass transition temperature of a film of thickness H, $T_g(H)$, decreases with decreasing H ($\Delta T_g < 0$).[16, 18, 20-23] Conversely, when the monomer-substrate interactions are strong, such as poly(methyl methacrylate) (PMMA) on SiO_x substrates, due to hydrogen-bonding between the polymer and the SiO_x, the average $T_g(H)$ increases with decreasing H ($\Delta T_g>0$).[11-15, 18, 22-24]

It was evident from the work of Kawana and Jones, who examined the PS/SiO_x system, that due to the existence of a low T_g surface layer, T_g^{surf}, the aging of the interior of the film would occur at a different rate than the free surface.[6, 8, 10, 25] Priestley *et. al*. subsequently showed that in the $PMMA/SiO_x$ thin film system, the aging rate decreased by factors of 2 and 15, at the free surface and substrate, respectively.[2] However, these measurements were only performed at a single aging temperature, where $\Delta T_A \sim -80°C$. The slow aging of the film was reconciled by considering that near the free surface the driving force is lower than the bulk because $(T_g^{surf} - T_{age}) < (T_g(H) - T_{age})$. Additionally, the reduction of the aging rate at the substrate stems from the reduced cooperative segmental mobility at the substrate.[2] Through a more extensive study of the PS/SiO_x system, over a wide range of aging temperatures, Pye *et. al.* showed that the physical aging rate of PS films of H=30 nm was slow, for all temperatures, relative to the

bulk.[6] They interpreted their observations by assuming the existence of a mobile surface layer of characteristic thickness, H_{FS}, which does not age; the remainder of the film aged at the rate of the bulk. The existence of a liquid-like surface layer, has been used to rationalize the thickness dependent behavior of T_g.[26, 27]

The differences between the chemical structures and associated differences between the monomer-interface interactions are responsible for the differences of the values of T_g^{surf} and $T_g(H)$ for PS/SiO_x and for PMMA/SiO_x. Therefore, in light of the foregoing discussion, it is not immediately obvious how to reconcile the fact that both PS/SiO_x and PMMA/SiO_x thin films age slowly compared to thicker films and to the bulk.

Recently it was shown that for star-shaped polystyrene, changes only in the functionality, f, (number of arms) and the degree of polymerization per arm, N_{arm}, of the macromolecule, would be associated with increases or decreases in T_g^{surf}, relative to the bulk.[28, 29] Notably, the magnitudes of these changes in $T_g(H)$ with H, for these star-shaped macromolecules, are of the same magnitude as those exhibited linear chain PS and PMMA macromolecules, on the same substrates. It follows that the behavior of the star-shaped polymer systems provides an opportunity to examine how changes in the local T_g would influence the aging of thin films, in the absence of the added complication of differences between chemical structures. Through a comprehensive study, involving experiments investigating a range of values of T_{age}, of samples of different f and N_{arm}, we show that films in this thickness regime age slowly, compared to thicker films. The aging rates of star-shaped macromolecules are, moreover, slow compared to their linear

PS analogs. We show that by accounting only for the dependence of the T_g as a function of depth, z, within thin films the slow physical aging behavior of all these systems may be reconciled in terms of a "universal" picture. This is noteworthy because it is now apparent that the aging rate in materials may be controlled by changes in the architecture and size of the macromolecule.

The physical aging of linear and star-shaped polystyrene (PS) macromolecular thin films of various thicknesses, H, where 50 nm < H < 1 micron, supported by silicon oxide substrates, were examined using *in situ* spectroscopic ellipsometry (SE) by monitoring the change in H at a constant $T_{age}<T_g$, with time.[30] Linear PS of molecular weight of M_w=152 kg/mol. (LPS-152K) and two 8-arm star-shaped PS macromolecules: one with M_{arm}= 10 kg/mol. (SPS-10K) and the other with 25 kg/mol. (SPS-25K), were investigated. The SPS-10K polymer was chosen because its T_g^{surf} and T_g^{subst} are appreciably higher than the bulk.[28] Recall, in contrast, that for linear chain PS, supported by the same substrates, T_g^{surf} is appreciably lower than the bulk and its T_g^{subst} is comparable to the bulk. The T_g^{surf} of the SPS-25K sample is comparable to its bulk value whereas its T_g^{subst} is slightly higher than the bulk. In short, we investigate the behavior of three systems of the same chemical structure, but different architecture, and consequently very different interfacial and bulk T_gs.

Ellipsometry measurements of the normalized thickness, $H(t_{age})/H(t_{age}=10)$, dependencies on time, t_{age}, for LPS-152K and SPS-10K films and for two different thicknesses are shown in Fig. S1.[30] The thinner film (initial thicknesses H_0~50 nm) exhibits a weaker dependence on time than the thicker (H_0~1100 nm) film. Note that in

this figure, $t_{age} = t - t_0$ is plotted instead of t, since during the initial stage of any aging experiment the thickness is constant in this so-called initial plateau regime.[10] The width of the plateau region increases with decreasing T_{age}.[7, 31] The physical aging rate exhibits a logarithmic dependence on time and is well described by:

$$\beta = (-1/H_\infty)\, dH(t_{age}) / d(\log t_{age}) \qquad 1.$$

where H_∞ is the "equilibrium" film thickness.[5] We note that the aging rate of the LPS-152K system is consistent with the data previously described by Pye *et. al*., who also studied the aging of linear PS.[6]

The physical aging rates, calculated using equation 1, are plotted in Fig. 1 as a function of $\Delta T_A = T_{age} - T_g$. It is evident from these data that the physical aging rates of the thinner (51± 1 nm) films is slower than those of thick films, for all three systems (data for SPS-25K is shown in Fig. S2).[30] Additionally, it is evident from Fig. 2, where data for different thicknesses are included, that the aging rates of the star-shaped macromolecules exhibit stronger thickness dependencies than their linear chain analogs (see additional data in Fig. S3).[30] The differences between the physical aging behavior of the linear and star-shaped macromolecules cannot be reconciled entirely in terms of T_g^{surf} and $T_g(H)$. The aging rates may however be reconciled in terms of a model that accounts for the changes in the local T_g as a function of depth, $L_g(x)$, of the films. Knowledge of the $L_g(x)$ profile for a polymer film would enable calculation of the *local* aging rate, $\beta(x)$. As discussed below, $L_g(x)$ may be computed from experimentally measured thickness dependence of $T_g(H)$.[18] From the $L_g(x)$ profile, the average aging rate, β, for a film of

thickness H can be extracted; this will be compared directly with the experimental data in Fig.1 for the thinner films (H~50 nm), with no additional fitting parameters.

We first proceed by fitting the experimental data for the thick film, H~1 micron, using an empirical quadratic equation: $\beta(\Delta T_A)=a(\Delta T_A)^2+b(\Delta T_A)+c$, where $\Delta T_A=T_{age}-T_g(H)$; $T_g(H)$ is identically T_g^{film}. The solid lines, drawn through the thick film data (filled symbols) in Fig. 1, were computed using this equation. The connection between $T_g(H)$ and $L_g(x)$ is determined by considering the film to be composed of a large number of layers, each located a distance x away from the free surface. Each layer is characterized by a single T_g, $L_g(x)$; in the limit of an infinitesimal layer thickness $L_g(x)$ is treated as a smooth and continuous function. So the average T_g of a film may be defined such that

$$T_g(H) = \int_0^H L_g(x)dx \Big/ \int_0^H dx \qquad 2.$$

Experimentally it is well established that for thin films the thickness dependence of T_g scales inversely as $1/H$.[16, 17, 20, 26] This is also supported by theory.[14, 15, 19] Models based on dynamic percolation also lead to the same conclusion.[12, 13] Consequently, following Kim et al. the following relation for $T_g(H)$, is used:[18]

$$1/T_g(H) = \xi/T_g^{\infty} \cdot 1/H + 1/T_g^{\infty} \qquad 3.$$

where ξ is a measure of the influence of the interfacial interactions influence T_g^{surf}. Physically, ξ is a length scale that characterizes the distance from the free surface to the interior of the film where the half the bulk glass transition temperature, T_g^{∞}, is recovered. This parameter is not temperature dependent. Kim *et. al.* showed that for the non-wetting

case, such as for PS on SiO_x that $T_g^{surf}<T_g^{\infty}$ and that $T_g^{\infty}\approx T_g^{subst}$. It follows from equations 2 and 3 that $L_g(x) = T_g^{\infty} \cdot x(2\xi + x)/(\xi + x)^2$.[18] Using the published experimental data for $T_g(H)$ for the samples whose aging behavior is described in Fig. 2, $L_g(x)$ was calculated and plotted in Fig. 3.[28, 29] Details describing these calculations are provided in the section containing Supplemental Information.[30] It is evident that $L_g(x)$ of the linear chain system is smallest near the free surface and increases with x before reaching a plateau at T_g^{∞}=99°C, a value dictated by our experimental data. The value of $L_g(x\approx0)$ was also determined from our published data.[28, 29] The plateau in the figure is expected, based on all the available experimental data for the T_g of linear chain PS. The dependence of $L_g(x)$ for the SPS-25K sample is similar to that of the linear chains in the vicinity of the free surface; however $L_g(x)$ increases at the substrate. The situation involving SPS-10K is different; $L_g(x)$ is highest at both interfaces, as shown experimentally, and is independent of thickness in the middle of the film. This is in agreement with the experimentally determined local T_gs of this sample, measured using variable energy positron annihilation lifetime spectroscopy (PALS), at the free surface, and atomic force microscopy, at the substrate interface.[28, 29] The PALS data are plotted in the inset of Fig. 3; the agreement between the calculations of the model and experimental data is good. Additional results, calculated, using Eq. 2, as a function of H are compared with experimental data and plotted in Fig. S4, (see supplemental material).[30]

The next step is to calculate the local aging rate, $\beta(x)$, for each sample, based on $L_g(x)$; this enables calculation of the average aging rates of the H~50 nm samples and therefore a direct comparison with the experimental data in Fig 1. With the use of the empirical fitting parameters, a, b and c, from the quadratic equation, and replacing T_{age}-T_g with T_{age}-$L_g(x)$, the local aging rates for LPS-152K and SPS-10K were calculated and plotted in Fig. 4. For the linear PS system, the aging rate at the free surface is zero, because $T_{age} > T_g^{surf}$. Interestingly, for specific T_{age}, $\beta(x)$ exhibits a maximum for depths close to the interfaces. This may be rationalized in terms of the gradient in the local T_g close to the interfaces and, moreover, the non-monotonic dependence of aging rate on T_{age}. Since $\beta(T_{age})$ is in general not monotonic, then the assumption of an exponential decay in aging rate is not always appropriate.[6]

It is also apparent from the data in Figures 4A and 4B that the depth within the film at which the aging rate reaches zero, H_{FS}, is dependent on temperature. In the case of linear PS and SPS-25K, H_{FS} is a measure of the mobile free surface layer thickness. This layer does not age since $T_{age} > L_g(x)$. H_{FS} is shown to increase with increasing temperature, Fig. 4C. It is important to note that one consequence of using the 2-layer model is that H_{FS} is predicted to increase with decreasing temperature. This is not only in contrast to our findings; it is also not in agreement with recent studies by Paeng and Ediger on linear chain systems.[6, 32-34] In the case of SPS-10K, $\beta(x)$ reaches zero at both interfaces. This is of course not because $T_{age} > L_g(x)$, but due to the fact that $L_g(x)$ >> T_{age}. Since $L_g(x)$ is significantly larger than T_{age}, $\beta(x)$ is essentially zero due to the

reduced cooperative segmental mobility of the adsorbed layer, in line with a physical argument by Priestley *et*. *al*.[2]

Finally, we now reconcile these results with the experimental data in Fig. 1. Specifically, we calculate the average physical aging rates from the data in Fig. 4 and compare them to the experimental data in Fig. 1, for the H~50 nm films. To this end we consider a sample composed of infinitesimally thin films, each exhibiting a specific aging rate. With this, the average physical aging rate for a film, $\beta(H, T_{age})$ may be defined:

$$\beta(H, T_{age}) = \int_0^H \beta(T_{age} - L_g(x))dx / \int_0^H dx \qquad 4.$$

The broken lines drawn through the data in Fig. 1 were computed using the above equation; the agreement is very good. Clearly, the physical aging of the star and linear macromolecular thin films is extremely well described by the model that accounts solely for local changes in the *glass transition temperature,* $L_g(x)$, of the film. It is apparent from this assessment that it is imperative to account for both the local T_{age}-$L_g(x)$ and the bulk T_{age}-T_g. It is noteworthy that our analysis reveals that the characteristic length scale over which interfaces can influence the average aging rate may be as small as a few nanometers or as large as few hundreds of nanometers, depending on T_{age}-$L_g(x)$, or the bulk T_{age}-T_g, Fig. 2.[2, 6]

In conclusion, we showed that the average physical aging rate of supported polystyrene films of varying architectures is significantly slower than the bulk. Regions of the films in proximity to interfaces age at substantially different rates. This difference in aging rate of thin films is reconciled in terms of differences between local glass

transition temperatures, $L_g(x)$, and T_{age}. Additionally, it was demonstrated that the aging rates of the star-shaped macromolecules depends on the functionality and arm length of the macromolecule. The star-shaped macromolecules of sufficiently high functionality, and low M_{arm}, age more slowly than their linear chain analogs because they possess higher interfacial T_g's; in other words T_{age}-T_g(bulk) < T_{age}-T_g(interface). To this end, we have shown that the aging rates of thin films may be reconciled in terms of a universal picture that accounts for differences between T_{age} and the local glass transition temperature, $L_g(x)$. The results of this study indicate that the physical aging rates of thin polymer films may be tailored by controlling the molecular architecture. The macromolecular/interfacial interactions are sensitive to the architecture of the molecule, due primarily to entropic effects.

Support for this research from the National Science Foundation (NSF), Division of Material Research, Polymer Program No. 0906425 is gratefully acknowledged. We thank Richard Robertson for fruitful discussions.

REFERENCES

[1] L. C. E. Struik, *Physical Aging in Amorphous polymers* (Elsevier Scientific Publishing Company, Amsterdam, 1978).
[2] R. D. Priestley, C. J. Ellison, L. J. Broadbelt, and J. M. Torkelson, Science **309**, 456 (2005).
[3] I. M. Hodge, Science **267**, 1945 (1995).
[4] J. M. Hutchinson, Prog. Polym. Sci. **20**, 703 (1995).
[5] E. A. Baker, P. Rittigstein, J. M. Torkelson, and C. B. Roth, J. Polym. Sci. Pt. B-Polym. Phys. **47**, 2509 (2009).
[6] J. E. Pye, K. A. Rohald, E. A. Baker, and C. B. Roth, Macromolecules **43**, 8296 (2010).
[7] R. Greiner, and F. R. Schwarzl, Rheol. Acta **23**, 378 (1984).
[8] R. D. Priestley, L. J. Broadbelt, and J. M. Torkelson, Macromolecules **38**, 654 (2005).
[9] A. J. Kovacs, J. J. Aklonis, J. M. Hutchinson, and A. R. Ramos, J. Polym. Sci. Pt. B-Polym. Phys. **17**, 1097 (1979).
[10] R. D. Priestley, Soft Matter **5**, 919 (2009).
[11] J. Baschnagel, and F. Varnik, J. Phys.-Condes. Matter **17**, R851 (2005).
[12] J. E. G. Lipson, and S. T. Milner, Eur. Phys. J. B **72**, 133 (2009).
[13] D. Long, and F. Lequeux, Eur. Phys. J. E **4**, 371 (2001).
[14] J. Mittal, P. Shah, and T. M. Truskett, J. Phys. Chem. B **108**, 19769 (2004).
[15] T. M. Truskett, and V. Ganesan, J. Chem. Phys. **119**, 1897 (2003).
[16] J. L. Keddie, R. A. L. Jones, and R. A. Cory, Europhys. Lett. **27**, 59 (1994).
[17] J. A. Forrest, and K. Dalnoki-Veress, Adv. Colloid Interface Sci. **94**, 167 (2001).
[18] J. H. Kim, J. Jang, and W. C. Zin, Langmuir **17**, 2703 (2001).
[19] H. Morita, K. Tanaka, T. Kajiyama, T. Nishi, and M. Doi, Macromolecules **39**, 6233 (2006).
[20] J. L. Keddie, R. A. L. Jones, and R. A. Cory, Faraday Discuss. **98**, 219 (1994).
[21] C. J. Ellison, and J. M. Torkelson, Nat. Mater. **2**, 695 (2003).
[22] J. Q. Pham, and P. F. Green, J. Chem. Phys. **116**, 5801 (2002).
[23] J. Q. Pham, and P. F. Green, Macromolecules **36**, 1665 (2003).
[24] J. H. vanZanten, W. E. Wallace, and W. L. Wu, Phys. Rev. E **53**, R2053 (1996).
[25] S. Kawana, and R. A. L. Jones, Eur. Phys. J. E **10**, 223 (2003).
[26] J. A. Forrest, and J. Mattsson, Phys. Rev. E **61**, R53 (2000).
[27] J. Mattsson, J. A. Forrest, and L. Borjesson, Phys. Rev. E **62**, 5187 (2000).
[28] E. Glynos, B. Frieberg, H. Oh, M. Liu, D. W. Gidley, and P. F. Green, Phys. Rev. Lett. **106**, 128301 (2011).
[29] E. Glynos, B. Frieberg, and P. F. Green, Phys. Rev. Lett. **107**, 118303 (2011).
[30] See Supplemental Material at [URL will be inserted by publisher] for a description of the experiments and addition experimental data for SPS-25K and a more detailed description of the gradient Tg model.

[31] V. M. Boucher, D. Cangialosi, A. Alegria, J. Colmenero, J. Gonzalez-Irun, and L. M. Liz-Marzan, Soft Matter **6**, 3306 (2010).
[32] K. Paeng, S. F. Swallen, and M. D. Ediger, J. Am. Chem. Soc. **133**, 8444 (2011).
[33] K. Paeng, and M. D. Ediger, Macromolecules **44**, 7034 (2011).
[34] M. Ilton, D. Qi, and J. A. Forrest, Macromolecules **42**, 6851 (2009).

FIGURE LEGENDS

FIG. **1** (color online). The physical aging rates at different T_{age} relative to the average T_g of the film for: (A) LPS-152K and (B) SPS-10K. The filled symbols are for a 1.1 micron thick film and open symbols for a 50 nm thin film. The solid lines represent quadratic fits to the 1.1 micron film. The broken lines were calculated using the gradient model, described in the text.

FIG. **2** (color online). The physical aging rate normalized by the bulk physical aging rate as a function of thickness at 50°C below the average T_g of the film for: LPS-152K (open squares), SPS-25K (open triangles) and SPS-10K (open circles).

FIG. **3** (color online). The distribution in local T_g (L_g) throughout a 50 nm supported film for LPS-152K (black, squares), SPS-25K (green, triangles) and SPS-10K (red, circles) according to a gradient T_g model. The inset shows the same L_g for a 350nm film, with the PALS results, reproduced from Ref. 28, overlaid.[28]

FIG. **4** (color online). The distribution in local physical aging rate throughout a 50 nm supported film of T_g-25°C (black), T_g-35°C (blue) and T_g-50°C (red) for (A) LPS-152K and (B) SPS-10K. (C) The thickness of the free surface layer that does not age for: LPS-152K (black), SPS-10K (red) and SPS-25K (blue).

FIG. 1

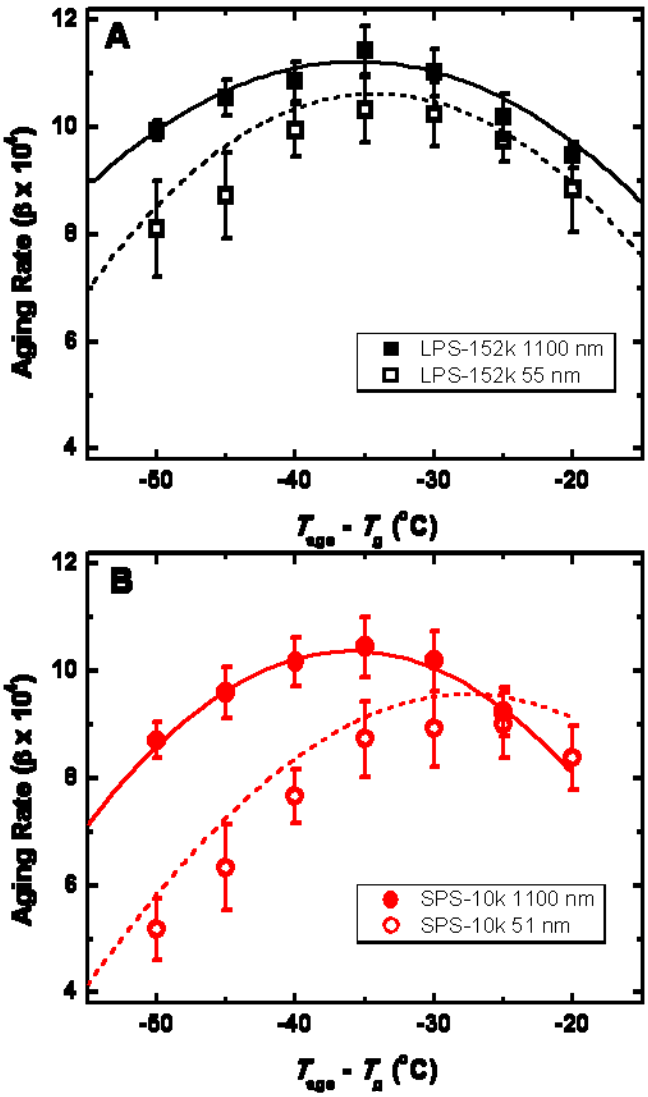
A
Aging Rate (β x 10⁴)
12
10
8
6
4
-60
-40
-30
-20
LPS-152k 1100 nm
LPS-152k 55 nm
T_age - T_g (°C)
B
Aging Rate (β x 10⁴)
SPS-10k 1100 nm
SPS-10k 51 nm
T_age - T_g (°C)

FIG. 2

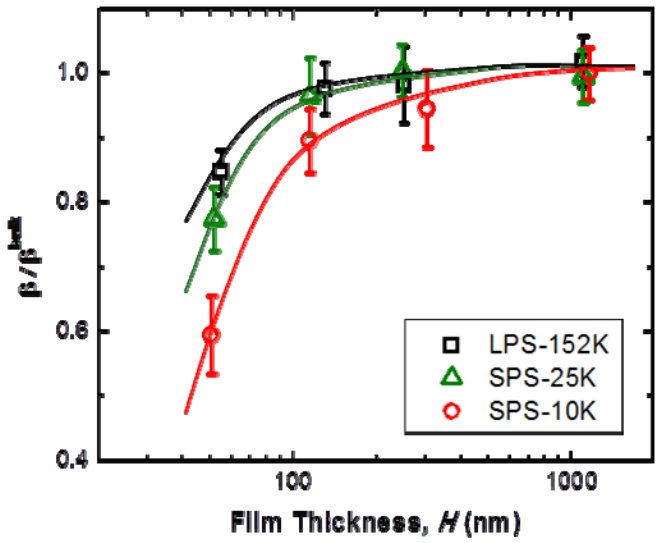
1.0
0.8
0.6
0.4
100
1000
Film Thickness, H (nm)
LPS-152K
SPS-25K
SPS-10K

FIG. 3

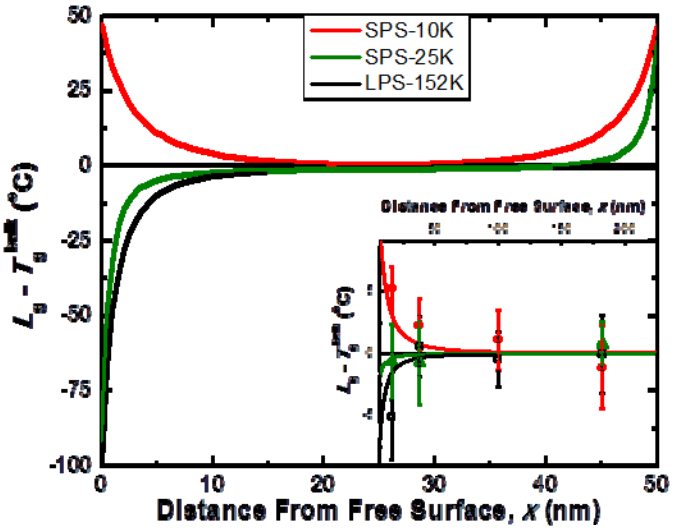
SPS-10K
SPS-25K
LPS-152K
50
25
0
-25
-50
-75
-100
0
10
20
30
40
50
Distance From Free Surface, x (nm)
$L_g - T_g^{bulk}$ (°C)

FIG. 4

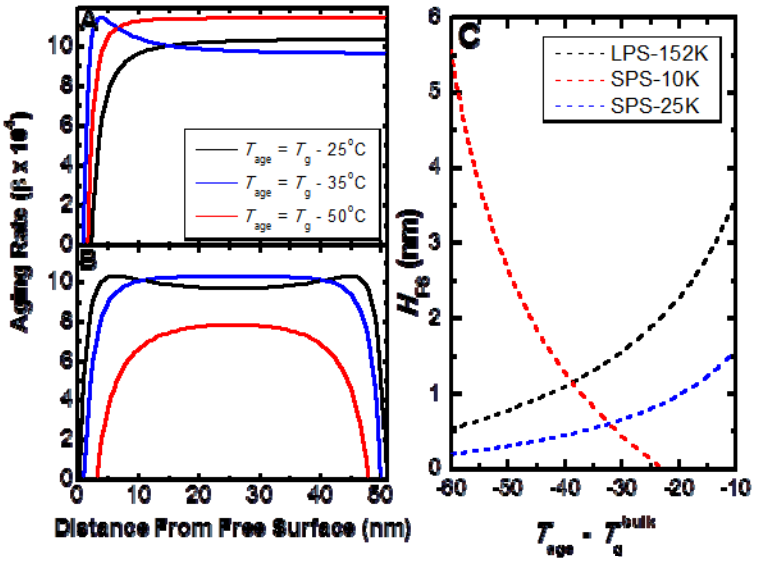
A
B
C
T_{age} = T_g - 25°C
T_{age} = T_g - 35°C
T_{age} = T_g - 50°C
Aging Rate (β x 10⁴)
Distance From Free Surface (nm)
LPS-152K
SPS-10K
SPS-25K
H_{Fs} (nm)
T_{age} - T_g^{bulk}